-RESEARCH PAPER-

International Journal of Mining and Geo-Engineering

IJMGE

IJMGE 56-3 (2022) 257-269

DOI: 10.22059/IJMGE.2022.306688.594858

Modeling of unconfined compressive strength and Young's modulus of lime and cement stabilized clayey subgrade soil using Evolutionary Polynomial Regression (EPR)

Ali Reza Ghanizadeh [a, *], Nasrin Heidarabadizadeh [a], Meysam Bayat [b], Vahid Khalifeh [a]

[a] *Department of Civil Engineering, Sirjan University of Technology, Sirjan, Iran.*

[b] *Department of Civil Engineering, Najafabad Branch, Islamic Azad University, Najafabad, Iran.*

Article History:

Received: 22 July 2020.

Revised: 02 October 2021.

Accepted: 05 March 2022.

ABSTRACT

In this study, the evolutionary polynomial regression (EPR) method has been employed to develop simple models with reasonable accuracy to predict the compressive strength and Young's modulus of the lime/cement stabilized clayey subgrade soil. For this purpose, the different specimens with the various cement and lime contents, at three moisture contents (dry side, wet side, and optimum moisture content) were fabricated and were cured for 7, 14, 21, 28, and, 60 days to conduct the unconfined compressive strength (UCS) test. According to the test results, a dataset consisting of 75 records for each additive was prepared. Results of this study show that the R^2 value of the developed model for predicting UCS of cement-stabilized clay soil is equal to 0.96 and 0.95 for training and testing sets, respectively. These two values for lime-stabilized soil are 0.91 and 0.87, respectively. Moreover, the R^2 for predicting Young's modulus of cement-stabilized clay soil is equal to 0.90 and 0.89 for the training and testing set, respectively. These two values for predicting Young's modulus of lime-stabilized soil are 0.88 and 0.94, respectively. The sensitivity analysis showed that for the Portland cement stabilized clayey subgrade, the percentage of the Portland cement and moisture content are the most significant parameters for predicting the UCS and Young's modulus, respectively. In contrast, for the lime-stabilized clayey subgrade soil, the most important parameters are the moisture content and the UCS, respectively.

Keywords: *Stabilized clay, Portland cement and lime, Unconfined compressive strength, Young's modulus, Evolutionary polynomial regression.*

1. Introduction

The rising costs of transportation and replacing low-quality materials have increased the use of the existing subgrade soils for road construction projects. However, the low bearing capacity often leads to some problems in using them. A variety of additives, such as lime, Portland cement, fly ash, bitumen emulsion, and polymer, may be used to improve the soil specifications. Soil stabilization will increase the strength and bearing capacity of the subgrade soils and reduces the pavement thickness.

The performance of an additive depends on the soil and field conditions. In recent years, many researchers have studied soil stabilization using a variety of additives, such as lime, cement, fly ash, and industrial wastes [1-10].

One of the first projects in which cement was used as a soil stabilizer was a construction project in South Carolina in 1935 [11]. The effects of cement stabilization with or without any additives on the performance of a wide range of soils have been evaluated by prior researchers [1; 12-18]. Previous research studies have shown that the treatment of clay soils with Portland cement decreases the liquid limit, plastic index, and swelling potential but increases the shrinkage limit and shear strength [19].

The cement can be used to stabilize a wide range of soils. However, the cement cannot be used for soils with an organic matter content greater than 2% or when the pH of the soil is lower than 5.3 [20]. The plasticity index of the cement-stabilized clay will decrease if the plastic limit increases. The cement content and curing time are two factors that affect the plastic limit [21]. The ACI 230 Committee report has stated that the cement changes some properties of soils, such as the maximum dry density and optimum moisture content. However, the direction of this change cannot be predicted. Moreover, cement stabilization leads to an immediate decrease in soil moisture [21].

Lime is also one of the additives that change soil properties. The soil stabilization with the lime reduces the liquid limit and plasticity index. The chemical reaction between the soil and lime also reduces the moisture content and maximum dry density but increases the optimum moisture content and bearing capacity of the soil [22]. Croft showed that some engineering properties of soils like the swelling potential, liquid limit, plasticity index, and maximum dry density would be significantly decreased and the optimum moisture content, shrinkage, and bearing capacity will be increased when using the lime as a stabilizer [23]. Bell found that the optimum lime content for soil stabilization is usually between 1 to 3 percent by weight of the soil, which does not change the plastic limit, but increases the strength [24]. However, the other studies reported a range of 2 to 8% for the lime stabilization of soils [25]. Ola and Gillot said that the stabilizer and soil type, soil minerals, and particle shape and size affect the soil stabilization results [26, 27].

Researchers have developed several models for predicting the unconfined compressive strength (UCS) and compaction parameters (maximum dry density and optimum moisture content) of the stabilized

* Corresponding author. Tel: +989126495932, *E-mail address:* ghanizadeh@sirjantech.ac.ir (A. Ghanizadeh).

geomaterials using various machine learning methods [6, 28-31]. Among these methods, artificial neural network (ANN), support vector machine (SVM), and gene expression programming (GEP) have been widely used.

Das et al. utilized the artificial neural network (ANN) and support vector machine (SVM) to predict the maximum dry density, and UCS of the cement stabilized soil. The input parameters of their model included the liquid limit, clay, sand, and gravel percentages, moisture content, and cement percentage. Results of their study showed that the accuracy of the SVM was more than the ANN [32]. Suman et al. used the functional networks (FN) method and multivariate adaptive regression splines (MARS) to predict the UCS and maximum dry density of the cement-stabilized soil. Their results showed the suitability of these two methods for predicting the UCS and maximum dry density [33]. Sathyapriya et al. used the ANN and regression analysis to predict the UCS of soil stabilized by industrial wastes. In this study, it was found that both methods can predict the UCS based on the soil properties. However, the ANN provides a more accurate prediction than the regression analysis [34]. Ghorbani and Hasanzadehshooiili applied a Back-Propagation Artificial Neural Network (BP-ANN) and Evolutionary Polynomial Regression (EPR) to predict the CBR and UCS of the lime, and micro-silica stabilized samples. The results showed that a BP-ANN method is a suitable tool for predicting the CBR and UCS in any condition [6].

Mozumder et al. evaluated the performance of the SVM regression method for estimating the UCS of a geopolymer stabilized clayey soil. The results showed that the SVM regression is suitable for predicting the UCS [35].

Alavi et al. predicted the optimum moisture content, maximum dry density, and UCS of the stabilized soils using an optimized linear genetic programming (LGP) method. The results showed that the LGP has lower accuracy than the hybrid LGP and simulated annealing LGP/SA method [36]. Gullu used genetic programming to predict the UCS, and Young's modulus of fly ash stabilized soil. In this study, the inputs were considered as the percentages of fly ash, dry unit weight, relative density, and energy absorption capacity. The results showed that the genetic programming was more accurate than the nonlinear regression to predict the UCS and Young's modulus [37]. Motamedi et al. used the adaptive neuro-fuzzy inference system (ANFIS) to predict the UCS of sandy soil stabilized with the pulverized fuel ash (PFA) and cement [38]. In another study, Motamedi et al. used the SVM and ANFIS to predict the UCS of the sand stabilized with the cement and cockleshell. The results showed the high accuracy of the ANFIS compared to the SVM [39]. Soleimani et al. used multi-gene genetic programming (MGGP) to predict the UCS of geopolymer-stabilized soils. The model presented in this study included several input parameters such as the ash percentage, slag furnace slag percentage, liquid limit, plastic limit, plasticity index, and molar concentration. The results showed that the proposed model could predict the UCS values with high accuracy [40].

Despite the high ability of artificial neural networks to record and represent the behavior of engineering systems, there are some shortcomings in this method and other machine learning methods such as support vector machines and adaptive fuzzy neural inference systems. For example, in the neural network, the number of hidden layers and the number of neurons in the hidden layer must be selected, for which the trial and error method is usually used. Another major drawback of these methods is related to the nature of the black box and the simple and interpretable relationship between inputs and outputs is not recognizable.

Evolutionary Polynomial Regression (EPR) is a new advanced regression method, that combines the best features of least square regression and the genetic programming regression techniques. The significant advantage of the EPR compared to other machine learning methods such as the ANN, SVM, and ANFIS is providing a simple and transparent equation for the prediction of the unknown parameters. Also, the required calculations for the other techniques are relatively complex and usually cannot be performed manually. The EPR has been successfully applied for modeling several geotechnical problems including stress-strain and volume change behavior of unsaturated soils [41], stability of soil and rock slopes [42], permeability, compaction characteristics of soil [43], flow number of asphalt mixtures [44], resilient modulus of fine subgrade soil [45], Hunched_Back Quay Wall [46], shallow foundations settlement [47], pullout capacity of anchors [47], ultimate bearing capacity of piles [47], UCS of Stabilized sandy soil, UCS and CBR of micro-silica-lime stabilized sulfate silty sand [48], and UCS of alkali-activated stabilized sandy soils [49].

Although extensive research has been conducted on cement and lime stabilization less attention has been paid to developing a model for predicting the UCS and Young's modulus of stabilized soils. Therefore, the main aim of this study is to develop a model to predict these two parameters using evolutionary polynomial regression (EPR). In addition, the gamma test method was used to determine the degree of importance of each input parameter on compressive strength and Young's modulus. Parametric analysis was also used to identify the effect of each of the input parameters on compressive strength and Young's modulus.

2. Evolutionary Polynomial Regression (EPR)

The EPR is a data mining hybrid regression method introduced by Giustolisi and Savic [50]. The EPR has two main steps. In the first step, the exponents of the symbolic model are selected using an evolutionary search strategy based on the genetic algorithm [51]. In the second step, the regression coefficients of the model (adjustable parameters) are determined using the least-squares method. The general form of the EPR model can be presented as follows [50]:

$$y = \sum_{j=1}^{m} F\left(X, f(X), a_j\right) + a_o \quad (1)$$

Where y is the estimated output vector, m is the number of polynomial terms, F is the extended function, X is the matrix of the input variables, f is a user-defined function, a_j is a constant, and a_0 is a bias term.

In the EPR, the least-squares method is used to determine the adjustable parameters. This method evaluates the adjustable parameters based on minimizing the sum of squared errors (SSE). Therefore the general form of the EPR is as follows:

$$\hat{y} = a_0 + \sum_{i=1}^{m} a_i (X_1)^{ES(i,1)} \dots (X_k)^{ES(k,1)} f\left((X_1)^{ES(i,k+1)}\right) \dots f\left((X_k)^{ES(i,2k)}\right) \quad (2)$$

$$\hat{y} = a_0 + \sum_{i=1}^{m} a_i f\left((X_1)^{ES(i,1)} \dots (X_k)^{ES(i,k)}\right) \quad (3)$$

$$\hat{y} = a_0 + \sum_{i=1}^{m} a_i (X_1)^{ES(i,1)} \dots (X_k)^{ES(i,k)} f\left((X_1)^{ES(i,k+1)} \dots (X_k)^{ES(i,2k)}\right) \quad (4)$$

$$\hat{y} = f\left(a_0 + \sum_{i=1}^{m} a_i (X_1)^{ES(i,1)} \dots (X_k)^{ES(i,k)}\right) \quad (5)$$

Where X_k is the k^{th} explanatory variable, $\hat{y}$ is the predicted value, k is the number of independent prediction variables (inputs), f is a function selected by the user, ES is the matrix of unknown parameters, and m is the number of polynomial terms, a_i is the model parameter, a_0 is a bias term. The internal functions of this model can be considered linear or nonlinear [52]. Figure 1 shows the EPR modeling process.

3. Experimental Program

3.1. Materials

The clay soil was collected from the northwest of the Markazi province of Iran. The soil properties are given in Table 1. The gradation curve and compaction test results according to ASTM D1557 are shown in Figures 2 and 3, respectively. The physical and chemical properties of the hydrated lime and Portland cement are also given in Table 2.

3.2. Preparing Specimens

The dry materials (soil and additive) were sufficiently mixed for 2 minutes to prepare the compacted cylindrical specimens (50 mm in diameter, 100 mm in height). Then the calculated amount of water was added. Mixed material was molded and compacted immediately into five equal layers using a steel hammer to obtain the maximum dry density. After the compaction process, the cylindrical specimens were

removed from the molds, and after weighing, they were cured at room temperature (approximately 25 ° C). It is noted that three specimens were prepared for each curing period. In this study, the specimens with 7, 14, 21, 28, and 60 days curing periods and different moisture contents (including the optimum moisture content, 2% more than the optimum moisture (wet side) and 2% less than the optimum moisture (dry side)) were prepared and cured.

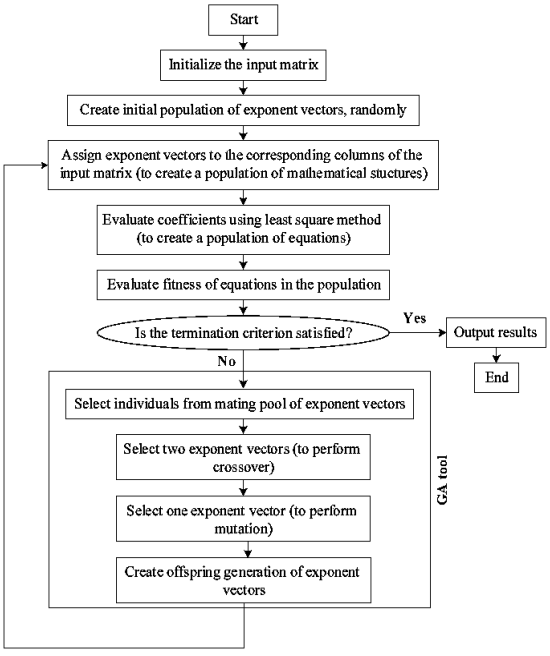

Figure 1: The EPR process flowchart [53].

3.3. Unconfined Compression Strength Test

The unconfined compression strength (UCS) test is commonly used for the mix design and quality control of stabilized materials and has been conducted for different geotechnical aspects by several researchers [1, 54- 57]. UCS is often used as an index to evaluate the performance (bearing capacity) of stabilized soil. In this study, the UCS test was performed under a constant strain rate (2% per minute), and the UCS, as well as Young's modulus (secant modulus), corresponding to the 50% of failure strain, were determined.

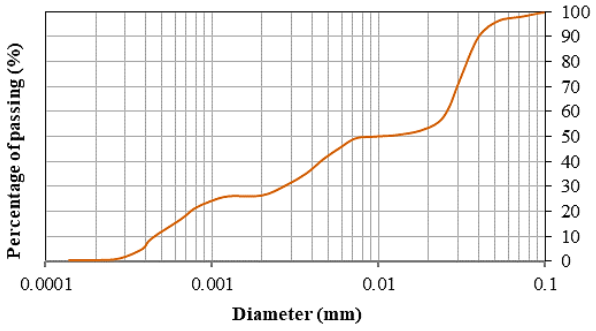

Figure 2. Soil gradation curve.

4. Datasets

In this study, two experimental datasets (75 data in each set) were used for developing EPR models to predict the UCS and Young's modulus of stabilized clay soil. In these two datasets, the percentage of cement or lime (%), moisture content (%), and curing time (days) were considered independent variables, and the UCS and Young's modulus were considered the dependent variables. The statistical data are presented in Tables 3 and 4. To better understanding the data distribution, the frequency diagrams of the variables for both datasets are shown in Figure 4.

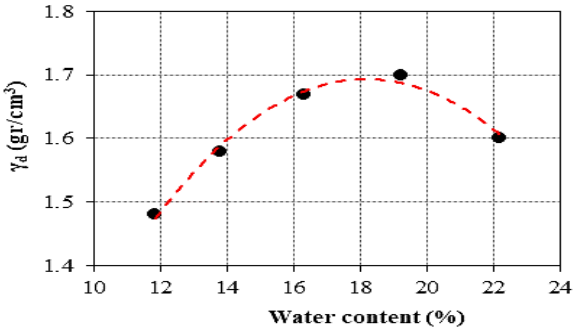

Figure 3. Standard proctor compaction Curve.

Table 1. The Geotechnical properties of soil

parameter	value
Liquid limit (%)	29
Plastic limit (%)	20
Plasticity index (%)	9
Maximum dry density (gr/cm³)	1.7
Optimum moisture content (%)	18.5
The specific gravity (Gs)	2.6
$P_{\#200}$ (%)	98
Unified Soil Classification	CL
AASHTO Soil classification by AASHTO	A4

Table 2. The Chemical and physical properties of Portland cement and hydrated lime.

Properties	Hydrated lime	Portland cement
Bulk density (Kg/Cm³)	490	1380
The specific gravity (Gs)	2.35	3.15
Specific surface area (cm²/g)	-	2900
CaO (%)	-	61.3
$Ca(OH)_2$ (%)	96	-
SiO_2 (%)	-	15.3
MgO (%)	-	0.9
$Mg(OH)_2$ (%)	0.5	-
Al_2O_3 (%)	-	9.3
$CaCO_3$ (%)	1.5	-
$CaSO_4$ (%)	0.03	-
Fe_2O_3 (%)	-	4.2
K_2O (%)	-	0.8
TiO_2 (%)	-	0.1
SO_3 (%)	-	6.4

5. Developing the prediction model of the compressive strength and Young's modulus based on the Evolutionary Polynomial Regression (EPR)

In this section, the procedure and details of modeling based on the EPR method for predicting the UCS and Young's modulus of cement/lime stabilized clay will be described. To this end, the EPR MOGA-XLvr.1 software was employed [58]. For validating the EPR models, 70% (53 records) and 30% (22 records) of the data were randomly selected as the training and testing sets, respectively. The range of variation and statistical limits of these two datasets are presented in Tables 5 and 6 for the samples stabilized with the Portland cement and lime, respectively. For the prediction of the UCS, the cement/lime percentage (CC or LC), moisture content (MC), and curing time (CT) were considered as the input variables, and the UCS (kPa) was considered as the output. However, for predicting Young's modulus, the cement/lime percentage (CC or LC), moisture content (MC), curing time (CT), and UCS were

considered as the input variables, and Young's modulus corresponding to the 50% of failure strain in kPa (E50) was considered as the output variable. To develop the EPR model, different models were developed assuming different values for the EPR setting parameters and finally, the optimum value of parameters was determined. Table 7 shows the optimum value of the EPR parameters.

Table 3. The statistical characteristics of laboratory data for the cement-stabilized clay.

Variable	Maximum	Minimum	Average	Standard deviation	Median
Cement (%)	9	0	4.8	3.145	5
Moisture (%)	22.65	16.4	19.37	1.86	19.3
Curing time (day)	60	7	26	18.509	21
UCS (kPa)	5360	295	2113.493	1253.199	2038
E50 (kPa)	700	3	220.67	185.28	150

Table 4. The statistical characteristics of laboratory data for the lime-stabilized clay.

Variable	Maximum	Minimum	Average	Standard deviation	Median
Lime (%)	9	0	4.8	3.145	5
Moisture (%)	22.6	16.5	21.3	2.647	21.2
Curing time (day)	60	7	26	18.509	21
UCS (kPa)	1450	220	685.587	292.546	610
E50 (kPa)	257	3	41.96	58.07	20.1

Table 5. The statistical parameters related to the cement-stabilized clay dataset.

Training data set (53 data)					
Variable	**Maximum**	**Minimum**	**Mean**	**Standard deviation**	**Median**
Cement (%)	9	0	4.91	3.2	5
Moisture (%)	24.78	14.72	19.27	3.23	18.5
Curing time (day)	60	7	26.79	19.21	21
UCS (kPa)	5360	361	2153.42	1280.32	2067
E50 (kPa)	700	3	220.57	181.64	130
Test data set (22 data)					
Variable	**Maximum**	**Minimum**	**Mean**	**Standard deviation**	**Median**
Cement (%)	9	0	4.55	2.92	5
Moisture (%)	24.78	14.72	19.62	3.93	19.3
Curing time (day)	60	7	24.09	16.06	21
UCS (kPa)	4500	295	2017.32	1149.12	1840
E50 (kPa)	700	3.5	220.91	193.78	175.4

Table 6. The statistical parameters related to the lime-stabilized clay dataset.

Training data set (53 data)					
Variable	**Maximum**	**Minimum**	**Mean**	**Standard deviation**	**Median**
Lime (%)	9	0	4.98	3.037	5
Moisture (%)	29.52	14.8	21.11	4.21	20
Curing time (day)	60	7	24.72	17.53	21
UCS (kPa)	1300	220	703.08	295.24	620
E50 (kPa)	300	3	50.42	58.89	24.4
Test data set (22 data)					
Variable	**Maximum**	**Minimum**	**Mean**	**Standard deviation**	**Median**
Lime (%)	9	0	4.36	3.283	5
Moisture (%)	29.52	14.8	21.76	3.62	22.2
Curing time (day)	60	7	29.09	19.96	21
UCS (kPa)	1450	270	643.45	274.527	600
E50 (kPa)	257	3	50.4	41.55	13.6

Table 7. The optimum value of the EPR parameters.

Description of parameter	Setting of parameters	
	UCS	**E_{50}**
Function set	logarithm	Secant Hyperbolic
Type of model	Statistical Regression	Statistical Regression
Type of presentation	$Y= sum(a_i*X_1*X_2*f(X_1*X_2))+a_0$	$Y= sum(a_i*X_1*X_2*f(X_1*X_2))+a_0$
Exponents range	[0.5, 1, 1.5, 2, -0.5, -1, -1.5, -2]	[0.5, 1, 1.5, 2, -0.5, -1, -1.5, -2]
Number of mathematical terms	5	5
Bias (a0) value	0	0

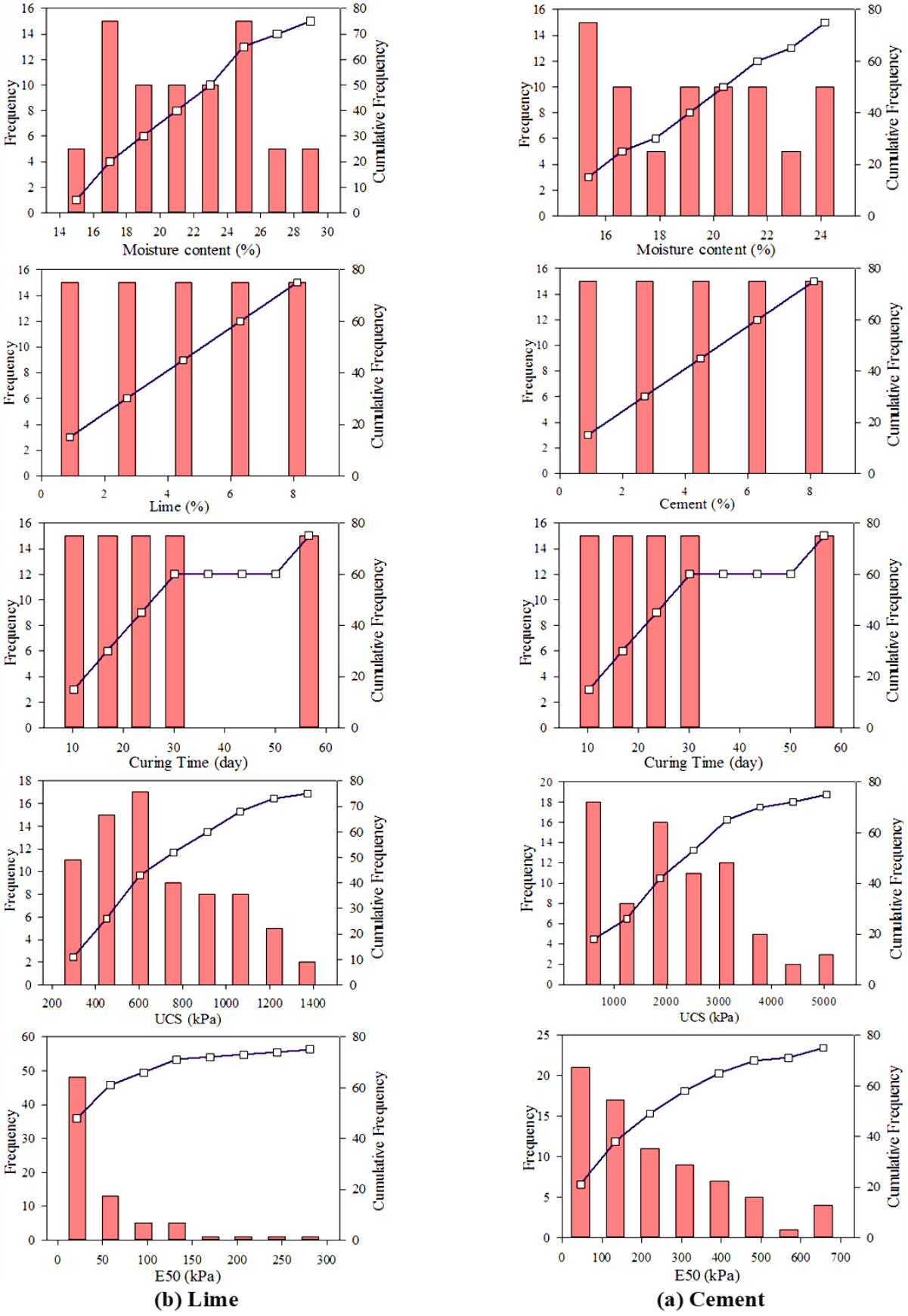

Figure 4. The frequency histogram for each of the variables.

The optimal EPR model for predicting the UCS and Young's modulus for the cement-stabilized clay (CUCS and CE_{50}) and lime-stabilized clay (LUCS and LE_{50}) were obtained according to equations (6) to (9).

$$CUCS = \frac{1869.9003}{MC^{0.5}} \cdot Ln(MC^{1.5}) + 1335.2939 \cdot Ln\left(\frac{1}{MC^{0.5}}\right) + 4.0781 \cdot MC^{0.5} \cdot Ln\left(\frac{MC^{1.5} \cdot CT}{C^{0.5}}\right) + 596.8243 \frac{C^{1.5}}{MC} Ln(C^2 \cdot MC^{1.5} \cdot CT^2) + 118.1526 \frac{C^2}{MC^{0.5}} Ln\left(\frac{MC^{0.5}}{C^2 \cdot CT^{0.5}}\right) \quad (6)$$

$$CE_{50} = 0.0010105 \frac{UCS^2}{MC} \cdot sech\left(\frac{C^2}{MC}\right) + 16963941737.455 \cdot \frac{C^{0.5} \cdot UCS^{0.5}}{MC^2} sech(CT^{1.5}) + 0.0068308 \cdot C^{0.5} \cdot MC^2 \cdot sech\left(\frac{1}{MC^{1.5}}\right) + 45.6824 \cdot \frac{C \cdot UCS^{0.5}}{MC^{1.5} \cdot CT^{0.5}} \cdot sech\left(\frac{MC^{1.5}}{CT^{1.5}}\right) \quad (7)$$

$$LUCS = \frac{8773.4167}{MC^{1.5}} \cdot Ln(CT^2) + 26.2715 \frac{CT}{MC^{1.5}} Ln(L^{0.5}) + 903.9236 \frac{L^{0.5}}{MC^{0.5}} + 0.99189 \cdot L^2 \cdot Ln\left(\frac{1}{L^2 \cdot CT}\right) \quad (8)$$

$$LE50 = 1.0343 \times 10^{-5} \frac{UCS}{L^{0.5} \cdot MC^{0.5} \cdot CT^{1.5}} \cdot sech\left(\frac{MC^2}{UCS^{0.5}}\right) + 0.012654 \frac{UCS^2}{MC^{1.5} \cdot CT^{0.5}} \cdot sech\left(\frac{CT}{L^{1.5}}\right) + 0.00021749 \frac{UCS^2}{MC^{0.5}} \cdot sech\left(\frac{1}{L}\right) + 9212.6793 \frac{UCS^2}{CT^{1.5}} sech(UCS^{0.5}) + 0.008898 \cdot L^{1.5} \cdot UCS^2 \cdot sech\left(\frac{MC^2}{UCS^{0.5}}\right) \quad (9)$$

5.1. Performance of the developed models

The following statistical equations were used to compare and evaluate the performance of the models:

$$RMSE = \sqrt{\frac{1}{M}\sum_{i=1}^{M}(h_i - t_i)^2} \quad (10)$$

$$R^2 = \left[\frac{\sum_{i=1}^{M}(h_i - \bar{h}_i)(t_i - \bar{t}_i)}{\sqrt{\sum_{i=1}^{M}(h_i - \bar{h}_i)^2 \sum_{i=1}^{M}(t_i - \bar{t}_i)^2}}\right]^2 \quad (11)$$

$$MAD = \frac{\sum_{i=1}^{M}|h_i - t_i|}{M} \quad (12)$$

$$MAPE = \frac{\sum_{i=1}^{M}|h_i - t_i|}{\sum_{i=1}^{M} h_i} \times 100 \quad (13)$$

Where M is the number of data in each set, h_i is the calculated value of the i^{th} output, t_i is the predicted value of the i^{th} output, $\bar{h}_i$is the mean of h_i, and $\bar{t}_i$ is the mean of t_i. It was noted that, for an accurate prediction with no errors, the expected value of R^2 is equal to 1, and the RMSE, MAD, and MAPE are equal to zero. Therefore, the RMSE, MAD, and MAPE with the lower values show a better performance than the developed model. The performance of the EPR models for predicting the UCS and Young's modulus of the cement/lime stabilized clay for the training, and testing sets are demonstrated in Figures 5 to 8, respectively.

As can be seen, the R^2 of the EPR model for the UCS prediction of the cement stabilized clay for training and testing sets are 0.96 and 0.95, respectively. Moreover, the R^2 of the lime-stabilized UCS for the training and testing set are 0.91 and 0.87, respectively. It is also observed that the coefficient of determination of Young's Modulus prediction equation in the case of cement stabilized clay soil for training and testing set are 0.91 and 0.89, and in the case of lime stabilized clay soil are 0.88 and 0.94, respectively. The statistical results obtained from equations 10 through 13 are presented in Table 8.

6. Parametric Analysis

Time limits and high costs of laboratory experiments are two factors that make researchers reluctant to carry out laboratory studies. In most cases, evaluating the input variable effects on the output results needs fabrication and curing of a considerable number of specimens, which increases the required time and cost. By developing the models, in addition to evaluating the effects of input variables on the outputs (here, UCS and Young's modulus), the parametric analysis can also be conducted. In this study, the effect of the cement/lime percentage, optimum moisture content, and curing time on the UCS and Young's modulus of the stabilized clay soil have been investigated. For this purpose, the desired parameters were considered between the lowest and highest value, and other parameters were assumed to be equal to the mean values. Then, the UCS and Young's modulus were determined according to the variation of the desired parameter. It should be noted that in the parametric analysis for Young's modulus, due to the dependence of the UCS on the other parameters (the additive percentage, moisture content, and curing time), the compressive strength value is considered variable. Figures 9 and 10 illustrate the effects of the inputs on the UCS of the cement and lime stabilized clay oils, respectively.

As can be seen from the figures, in the cement-stabilized specimens, with increasing the cement percentage, the UCS was increased. In the lime-stabilized samples with increasing the lime percentage, the UCS increases up to a specific value and then decreases. It is also observed that by increasing the moisture content or decreasing the curing time for the cement and lime stabilized specimens, the UCS decreases. Goodarzi stated that the reason for the decrease in UCS in the presence of large amounts of lime is due to the complete dissolution of clay particles and the lack of sufficient silica and alumina in the system for the continuation of pozzolanic reactions. Under these conditions, free lime remains between soil particles, and its low friction and adhesion reduce UCS [59]. Past research, on the other hand, has shown that increasing the water-to-binder ratio as well as increasing the curing time will increase UCS [56, 60, 61]. The effect of the water-to-binder ratio is similar to that of Portland cement concrete, and increasing the curing time improves the pozzolanic reaction, resulting in greater UCS of the stabilized soil. Figures 11 and 12 show the effects of the inputs on Young's modulus of the cement/lime stabilized clay, respectively.

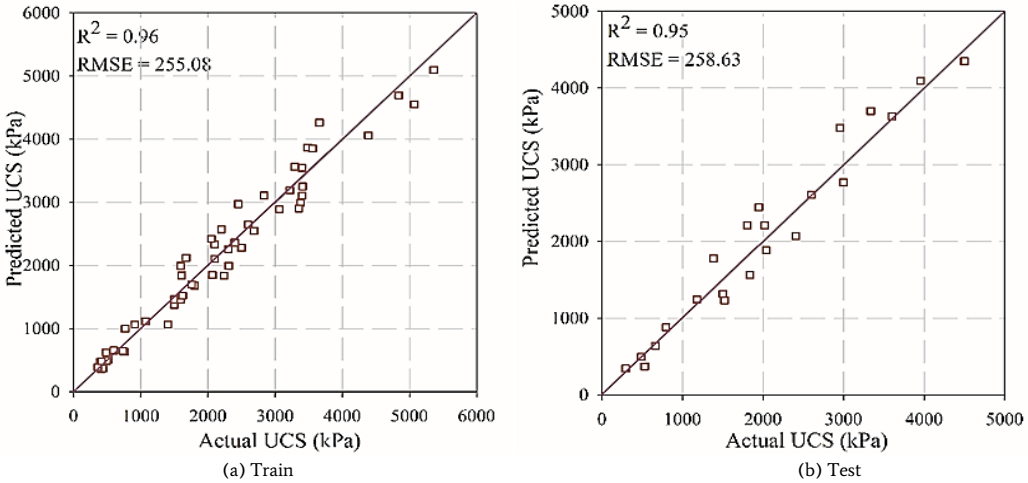

(a) Train (b) Test

Figure 5. The performance of the EPR model for predicting the UCS of cement stabilized clay soil.

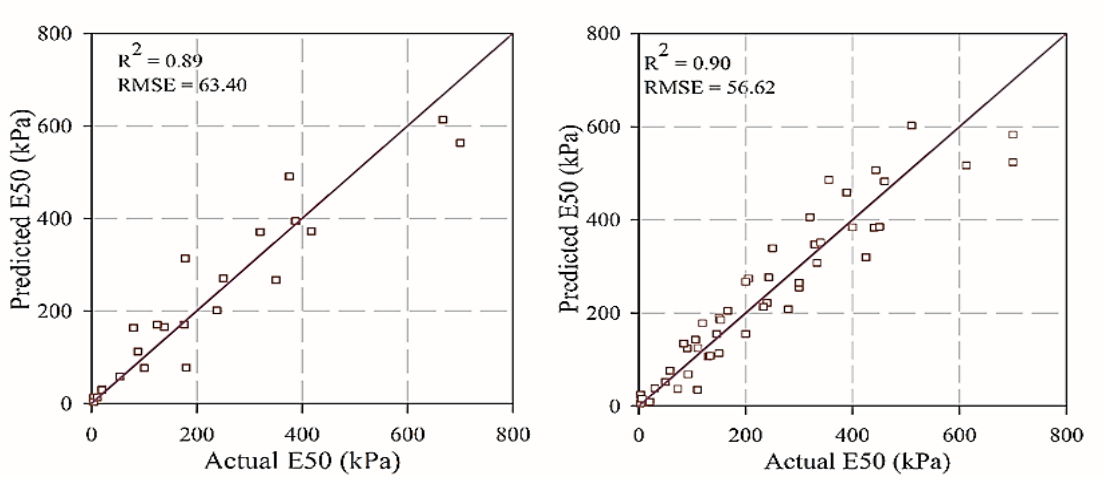

(a) Train (b) Test

Figure 6. The performance of the EPR model for predicting Young's Modulus of cement stabilized clay soil.

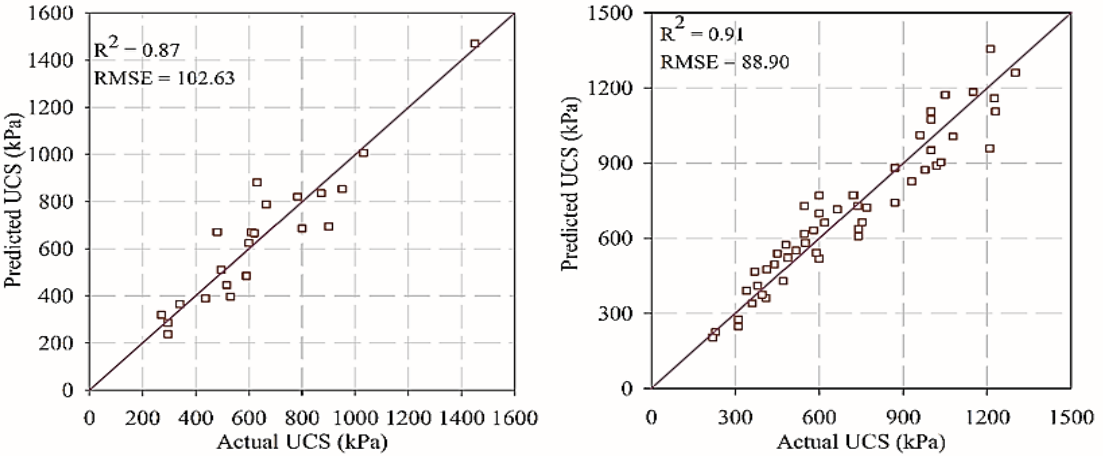

(a) Train (b) Test

Figure 7. The performance of the EPR model for predicting the UCS of lime stabilized clay soil.

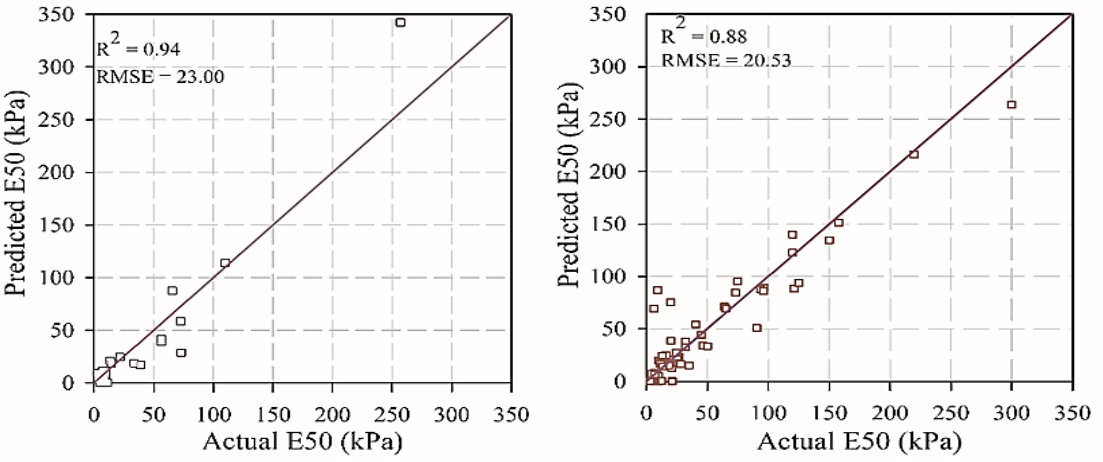

(a) Train (b) Test

Figure 8. The performance of the EPR model for predicting Young's Modulus of lime stabilized clay soil.

Table 8. Performance criteria for the developed EPR models.

Model		R^2	RMSE	MAD	MAPE
Cement stabilized UCS	Training	0.96	255.09	957.35	0.10
	Testing	0.95	258.63	822.85	0.10
	Total	0.96	256.13	979.34	0.10
Lime stabilized UCS	Training	0.91	88.90	186.46	0.10
	Testing	0.87	102.63	194.39	0.12
	Total	0.90	92.46	196.64	0.11
Cement stabilized Young's modulus	Training	0.90	56.62	144.85	0.20
	Testing	0.89	63.40	147.24	0.21
	Total	0.90	58.70	145.58	0.20
Lime stabilized Young's modulus	Training	0.88	20.53	35.73	0.26
	Testing	0.94	23.00	29.20	0.34
	Total	0.88	21.29	36.20	0.28

As expected, in the cement-stabilized samples, with increasing the cement percentage, Young's modulus increases, and in the lime-stabilized specimens, Young's modulus increases up to a certain value and then decreases. It is also observed that with increasing the moisture content or decreasing the curing time of the stabilized specimens, Young's modulus decreases. Moreover, with increasing the UCS of stabilized specimens, Young's modulus increases. As can be seen, the trend of changes in Young's modulus is similar to the trend of changes in uniaxial compressive strength, which is consistent with the results of other researchers [57, 62, 63].

7. Sensitivity Analysis Using Gamma Test

The Gamma Test (GT) can evaluate the relationship between the input and output variables. The GT calculates the minimum mean square error (MSE) using a smooth nonlinear function. For a better understanding of the GT, it is assumed that if the variables x and x' in the input space are closed together, their corresponding variables in the output space, y and y', will also be closed to each other. Otherwise, the noises have made a difference between them. Consider a set of parameters that are given as:

$$\{(x_i, y_i), 1 \le i \le M\} = (X, Y) \quad (14)$$

Where X is a vector, including the input variables x_i, and y_i are the corresponding output variables in the vector Y. The relationship between the x and y can be considered as:

$$y = f(x_1, \ldots, x_M) + r \quad (15)$$

In which r and f are random noise variables and the smooth function, respectively. The variance of the r can be calculated using the following equations:

$$\delta_M(k) = \frac{1}{M}\sum_{i=1}^{M}\left|x_{N(i,k)} - x_i\right|^2 \; 1 \le k \le p \quad (16)$$

$$\gamma_M(k) = \frac{1}{2M}\sum_{i=1}^{M}\left|y_{N(i,k)} - y_i\right|^2 \; 1 \le k \le p \quad (17)$$

Where $\gamma_M(k)$ is the Gamma function of the output variable, $\delta_M(k)$is the mean square distance to the k^{th} nearest neighbor, $x_{N(i,k)}$is the index of k^{th} nearest neighbor, $y_{N(i,k)}$is the corresponding output for $x_{N(i,k)}$, and |...| is the Euclidean distance. The best intercept of the linear regression line $\gamma_M(k)$, in contrast $\delta_M(k)$, is often named Γ. Therefore, by calculating Γ, the least-squares error can be obtained using the following equation:

$$\gamma = A\delta + \Gamma \quad (18)$$

If the vertical axis is intercepted (δ = 0), the value of Γ is shown as follows:

$$\gamma_M(k) \to Var(r) \quad as \quad \delta_M(k) \to 0 \quad (19)$$

When the Gamma value is zero, there will be no limit to developing a precise model, so the points with the lower gamma values will be used for modeling. The slope can also provide useful information. The slope is a dimensionless value indicating the complexity of the function. The standard deviation also expresses the accuracy of linear regression. It is more reliable if this value is closed to zero. Moreover, the V_{ratio} which returns the noise is calculated as:

$$V_{ratio} = \frac{\Gamma}{\sigma^2(y)} \quad (20)$$

Where, $\sigma^2(y)$ is the variance of y. In the gamma test, where the V_{ratio} is closer to zero, the y value is more accurate. However, for the input parameters which be resulted in V_{ratio} closer to 1, the value of random error is increased, and therefore, the extended model will be inappropriate.

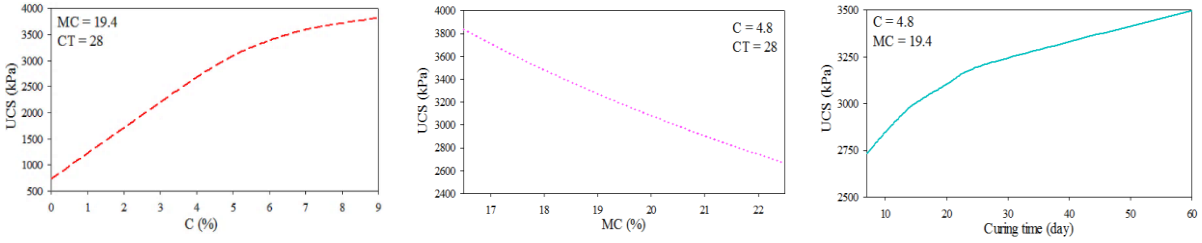

(a) Cement content (b) Moisture content (c) Curing time

Figure 9. The effect of input variables on the UCS of the cement-stabilized clay soil.

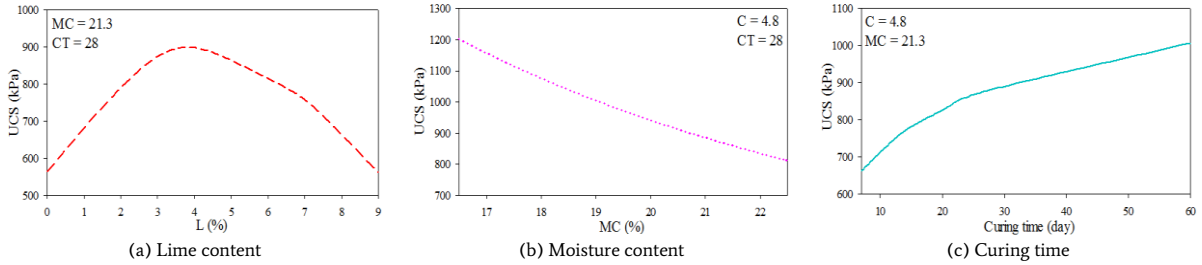

(a) Lime content (b) Moisture content (c) Curing time

Figure 10. The effect of input variables on the UCS of the lime-stabilized clay soil.

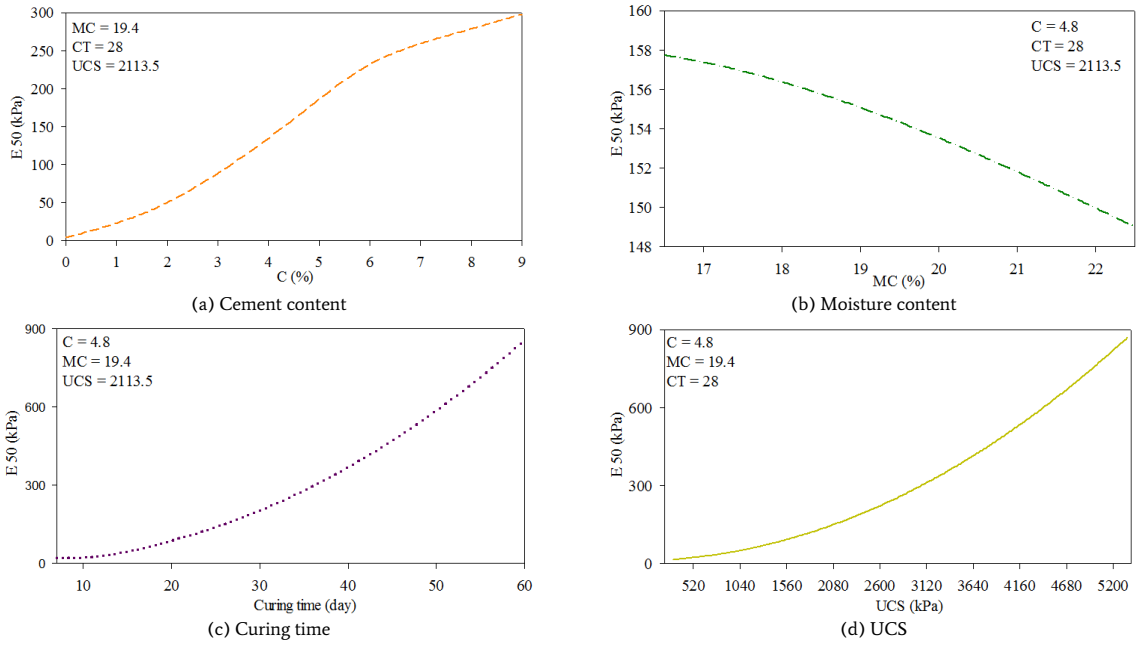

Figure 11. The effect of input variables on Young's modulus of the cement-stabilized clay.

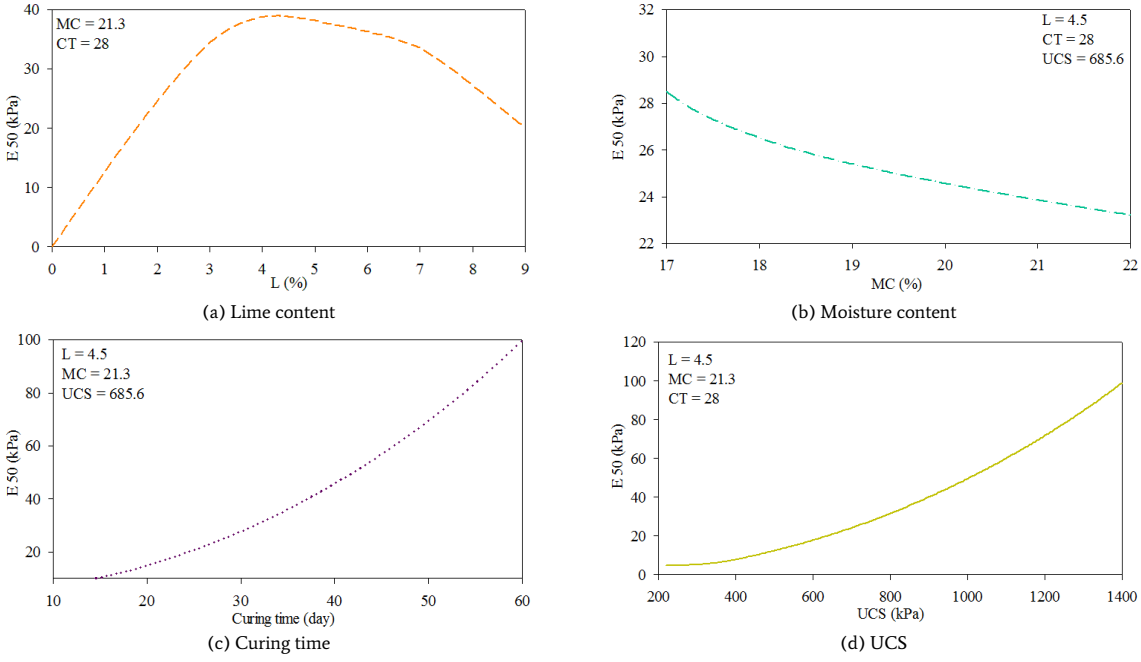

Figure 12. The effect of input variables on Young's modulus of the lime-stabilized clay.

Useful information can be obtained from the regression line of equation 17 and the distribution graph of the Gamma test in Figure 13. First, the y-intercept of the regression line shows the value of the Gamma test, which represents the portion of the output data variance that cannot be estimated by the model. Second, the slope of the regression represents the complexity of the model constructed from the input and output data. The steeper slope results in a more complex model.

In this study, the Gamma test was employed to determine the importance of input parameters affecting the UCS and E_{50}. Initially, the V_{ratio} was calculated considering all the parameters. In the subsequent scenarios, the input parameters were removed one by one, and the V_{ratio} was recalculated. Figures 14 and 15 show the effect of each scenario on the calculated V_{ratio} value for the two parameters UCS and E50. By increasing the model's sensitivity to the parameters, the V_{ratio} was increased. Therefore, the high value of the V_{ratio} can be used to identify the most influential parameters of the model.

As can be seen from the figures, the compressive strength of the cement-stabilized clay has the highest and lowest sensitivity to the Portland cement percentage and curing time, respectively. However, the

compressive strength of the lime-stabilized clay has the highest and lowest sensitivity to the moisture content and curing time, respectively. Moreover, Young's modulus of the cement-stabilized clay has the highest and lowest sensitivity to the moisture content and Portland cement percentage, respectively. However, Young's modulus of the lime-stabilized clay has the highest and lowest sensitivity to the compressive strength and curing time parameters, respectively.

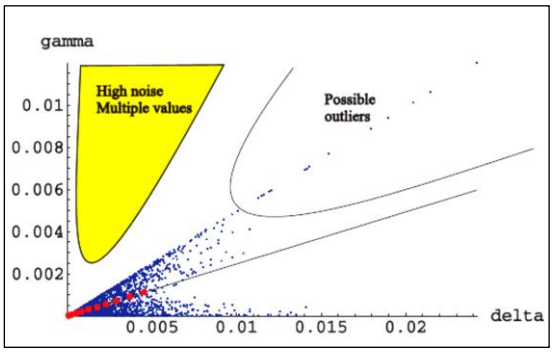

Figure 13. Distribution graph of the gamma test [64].

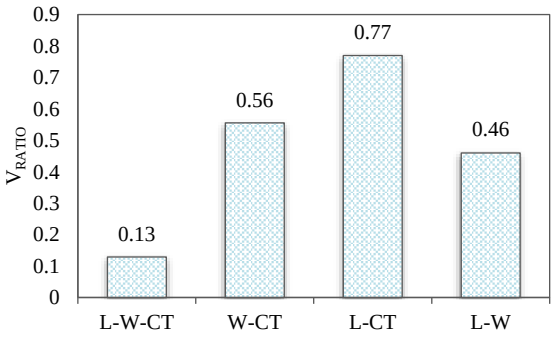

(a) Lime stabilized clay soil

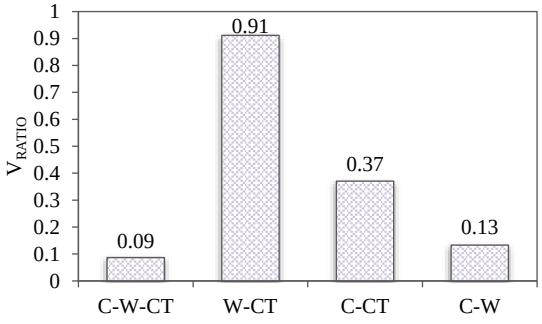

(b) Cement stabilized clay soil

Figure 14. Significant importance of the inputs for predicting the USC.

8. Conclusion

The results showed that the developed models based on the EPR have good accuracy in predicting the compressive strength and Young's modulus. So, in the cement-stabilized soils, the R^2 values related to the UCS prediction of the training and test data were 0.96 and 0.95 and for the lime-stabilized soils were 0.91 and 0.87, respectively. Moreover, in the cement stabilized soils, the R^2 values related to Young's modulus prediction of the training and test data were 0.90 and 0.89, and for the lime stabilized soils were 0.88 and 0.94, respectively. The results of the parametric analysis showed that in the cement-stabilized specimens, with increasing the cement percentage, the UCS increases.

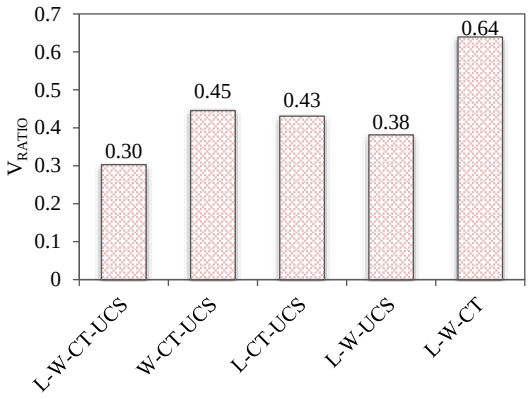

(a) Lime stabilized clay soil

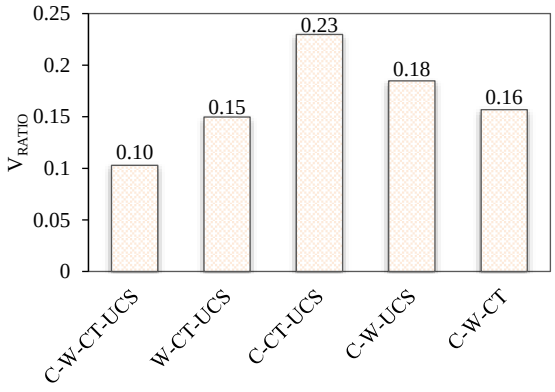

(b) Cement stabilized clay soil

Figure 15. Significant importance of the inputs for predicting Young's modulus.

The results showed that in the cement-stabilized soil, the cement percentage had the most impact and the curing time had the least impact on the compressive strength. However, in the lime-stabilized soil, the moisture content and curing time had the most and least impact on the UCS, respectively.

It should be noted that the moisture content had the most and the cement percentage had the least effect on the cement stabilized Young's modulus. However, the UCS and curing time had the most and least effect on Young's modulus of lime-stabilized soil, respectively. Due to the accuracy of the developed models, it can be concluded that the EPR method can be useful for solving complex geotechnical problems.

REFERENCES

[1] Yilmaz, Y., & Ozaydin, V. (2013). Compaction and shear strength characteristics of colemanite ore waste modified active belite cement stabilized high plasticity soils. Engineering Geology, 155(1), 45-53, DOI: 10.1016/j.enggeo.2013.01.003

[2] Anagnostopoulos, C. A. (2015). Strength properties of an epoxy resin and cement-stabilized silty clay soil. Applied Clay Science, 114(1), 517-529, DOI: 10.1016/j.clay.2015.07.007

[3] Zhao, Z., Hamdan, N., Shen, L., Nan, H., Almajed, A., Kavazanjian, E., & He, X. (2016). Biomimetic hydrogel composites for soil stabilization and contaminant mitigation. Environmental Science & Technology, 50(22), 12401-12410, DOI: 10.1021/acs.est.6b01285.

[4] Dang, L. C., Fatahi, B., & Khabbaz, H. (2016). Behaviour of expansive soils stabilized with hydrated lime and bagasse fibres. Procedia engineering, 143(1), 658-665, DOI:

10.1016/j.proeng.2016.06.093

[5] Furlan, A. P., Razakamanantsoa, A., Ranaivomanana, H., Levacher, D., & Katsumi, T. (2018). Shear strength performance of marine sediments stabilized using cement, lime and fly ash. Construction and Building Materials, 184(1), 454-463, DOI: 10.1016/j.conbuildmat.2018.06.231

[6] Ghorbani, A., & Hasanzadehshooiili, H. (2018). Prediction of UCS and CBR of microsilica-lime stabilized sulfate silty sand using ANN and EPR models; application to the deep soil mixing. Soils and foundations, 58(1), 34-49, DOI: 10.1016/j.sandf.2017.11.002

[7] Liu, L., Zhou, A., Deng, Y., Cui, Y., Yu, Z., & Yu, C. (2019). Strength performance of cement/slag-based stabilized soft clays. Construction and Building Materials, 211(1), 909-918, DOI: 10.1016/j.conbuildmat.2019.03.256

[8] Sharma, L., Sirdesai, N., Sharma, K., & Singh, T. (2018). Experimental study to examine the independent roles of lime and cement on the stabilization of a mountain soil: A comparative study. Applied Clay Science, 152(1), 183-195, DOI: 10.1016/j.clay.2017.11.012

[9] Söderlund, O., (2018) Stabilization of Soft Soil with Lime and PetritT. MSc Thesis, Luleå University of Technology.

[10] Yaghoubi, M., Shukla, S. K., & Mohyeddin, A. (2018). Effects of addition of waste tyre fibres and cement on the engineering behaviour of Perth sand. Geomechanics and Geoengineering, 13(1), 42-53, DOI: 10.1080/17486025.2017.1325941

[11] Das, BM. (1990). Principle of foundation engineering. USA, Boston

[12] Mohammadinia, A., Arulrajah, A., Sanjayan, J., Disfani, M. M., Bo, M. W., & Darmawan, S. (2014). Laboratory evaluation of the use of cement-treated construction and demolition materials in pavement base and subbase applications. Journal of Materials in Civil Engineering, 27(6), 04014186, DOI: 10.1061/(ASCE)MT.1943-5533.0001148

[13] Zhang, T., Yue, X., Deng, Y., Zhang, D., & Liu, S. (2014). Mechanical behaviour and micro-structure of cement-stabilised marine clay with a metakaolin agent. Construction and Building Materials, 73(1), 51-57, DOI: 10.1016/j.conbuildmat.2014.09.041

[14] Rios, S., Cristelo, N., Viana da Fonseca, A., & Ferreira, C. (2015). Structural performance of alkali-activated soil ash versus soil cement. Journal of Materials in Civil Engineering, 28(2), 04015125, DOI: 10.1061/(ASCE)MT.1943-5533.0001398

[15] Bekhiti, M., Trouzine, H., & Rabehi, M. (2019). Influence of waste tire rubber fibers on swelling behavior, unconfined compressive strength and ductility of cement stabilized bentonite clay soil. Construction and Building Materials, 208(1), 304-313, DOI: 10.1016/j.conbuildmat.2019.03.011

[16] Liu, Y., Wang, Q., Liu, S., ShangGuan, Y., Fu, H., Ma, B., Yuan, X. (2019). Experimental investigation of the geotechnical properties and microstructure of lime-stabilized saline soils under freeze-thaw cycling. Cold Regions Science and Technology, 161(1), 32-42, DOI: 10.1016/j.coldregions.2019.03.003

[17] Ghadir, P., & Ranjbar, N. (2018). Clayey soil stabilization using geopolymer and Portland cement. Construction and Building Materials, 188(1), 361-371, DOI: 10.1016/j.conbuildmat.2018.07.207

[18] Oluwatuyi, O. E., Adeola, B. O., Alhassan, E. A., Nnochiri, E. S., Modupe, A. E., Elemile, O. O., Akerele, G. (2018). Ameliorating effect of milled eggshell on cement stabilized lateritic soil for highway construction. Case Studies in Construction Materials, 9(1), e00191, DOI: 10.1016/j.cscm.2018.e00191

[19] Nelson, J., & Miller, D. J. (1997). Expansive soils: problems and practice in foundation and pavement engineering. John Wiley & Sons.

[20] ACI Committee, (1990) State-of-the-art report on soil cement. Journal ACI, 87(4), 395-417.

[21] Bergado, D., Anderson, L., Miura, N., & Balasubramaniam, A. (1996). Soft ground improvement in lowland and other environments. Bangkok, Thailand.

[22] Mallela, J., Quintus, H. V., & Smith, K. (2004). Consideration of lime-stabilized layers in mechanistic-empirical pavement design. The National Lime Association, 200(1), 1-40.

[23] Croft, J. (1967). The influence of soil mineralogical composition on cement stabilization. Geotechnique, 17(2), 119-135, DOI: 10.1680/geot.1967.17.2.119

[24] Bell, F. (1996). Lime stabilization of clay minerals and soils. Engineering geology, 42(4), 223-237, DOI: 10.1016/0013-7952(96)00028-2

[25] Basma, A. A., & Tuncer, E. R. (1991). Effect of lime on volume change and compressibility of expansive clays. Transportation research record, 1295(1): 52-61

[26] Ola, S. (1978). Geotechnical properties and behaviour of some stabilized Nigerian lateritic soils. Quarterly Journal of Engineering Geology and Hydrogeology, 11(2), 145-160, DOI: 10.1144/GSL.QJEG.1978.011.02.04

[27] Gillott, J. E. (2012). Clay in engineering geology. Elsevier, DOI: 10.1007/0-387-30842-3-9

[28] Ghanizadeh, A. R., & Rahrovan, M. Modeling of unconfined compressive strength of soil-RAP blend stabilized with Portland cement using multivariate adaptive regression spline. Frontiers of Structural and Civil Engineering, 13(4): 787-799, DOI: 10.1007/s11709-019-0516-8

[29] Manouchehrian, A., Sharifzadeh, M., & Moghadam, R. H. (2012). Application of artificial neural networks and multivariate statistics to estimate UCS using textural characteristics. International Journal of Mining Science and Technology, 22(2), 229-236, DOI: 10.1016/j.ijmst.2011.08.013

[30] Mozumder, R. A., & Laskar, A. I. (2015). Prediction of unconfined compressive strength of geopolymer stabilized clayey soil using artificial neural network. Computers and Geotechnics, 69(1), 291-300, DOI: 10.1016/j.compgeo.2015.05.021

[31] Torabi-Kaveh, M., Naseri, F., Saneie, S., & Sarshari, B. (2015). Application of artificial neural networks and multivariate statistics to predict UCS and E using physical properties of Asmari limestones. Arabian journal of Geosciences, 8(5), 2889-2897, DOI:10.1007/s12517-014-1331-0

[32] Das, S. K., Samui, P., & Sabat, A. K. (2011). Application of artificial intelligence to maximum dry density and unconfined compressive strength of cement stabilized soil. Geotechnical and Geological Engineering, 29(3), 329-342, DOI: 10.1007/s10706-010-9379-4

[33] Suman, S., Mahamaya, M., & Das, S. K. (2016). Prediction of Maximum Dry Density and Unconfined Compressive Strength of Cement Stabilised Soil Using Artificial Intelligence Techniques. International Journal of Geosynthetics and Ground Engineering, 2(2), 1-11, DOI: 10.1007/s40891-016-0051-9

[34] Sathyapriya, S., & Arumairaj, P. (2017). Prediction of Unconfined Compressive Strength of a Stabilised Expansive Clay Soil using ANN and Regression Analysis (SPSS). Asian Journal of

Research in Social Sciences and Humanities, 7(2), 109-123, DOI: 10.5958/2249-7315.2017.00075.2

[35] Mozumder, R. A., Laskar, A. I., & Hussain, M. (2017). Empirical approach for strength prediction of geopolymer stabilized clayey soil using support vector machines. Construction and Building Materials, 132(1), 412-424, DOI: 10.1016/j.conbuildmat.2016.12.012

[36] Alavi, A. H., Gandomi, A. H., & Mollahasani, A. (2012). A Genetic Programming-Based Approach for the Performance Characteristics Assessment of Stabilized Soil. In Variants of Evolutionary Algorithms for Real-World Applications, 343-376, DOI: 10.1007/978-3-642-23424-8_11

[37] Güllü, H. (2014). Function finding via genetic expression programming for strength and elastic properties of clay treated with bottom ash. Engineering Applications of Artificial Intelligence, 35(1), 143-157, DOI: 10.1016/j.engappai.2014.06.020

[38] Motamedi, S., Shamshirband, S., Petković, D., & Hashim, R. (2015). Application of adaptive neuro-fuzzy technique to predict the unconfined compressive strength of PFA-sand-cement mixture. Powder technology, 278(1), 278-285, DOI: 10.1016/j.powtec.2015.02.045

[39] Motamedi, S., Shamshirband, S., Hashim, R., Petkovic, D., & Roy, C. (2015). Estimating unconfined compressive strength of cockle shell-cement-sand mixtures using soft computing methodologies. Engineering Structures, 98(1), 49-58, DOI: 10.1016/j.engstruct.2015.03.070

[40] Soleimani, S., Rajaei, S., Jiao, P., Sabz, A., & Soheilinia, S. (2018). New prediction models for unconfined compressive strength of geopolymer stabilized soil using multi-gen genetic programming. Measurement, 113(1), 99-107, DOI: 10.1016/j.measurement.2017.08.043

[41] Javadi, A. A., Ahangar-Asr, A., Johari, A., Faramarzi, A., & Toll, D. (2012). Modelling stress-strain and volume change behaviour of unsaturated soils using an evolutionary based data mining technique, an incremental approach. Engineering Applications of Artificial Intelligence, 25(5), 926–933. DOI: 10.1016/j.engappai.2012.03.006

[42] Ahangar-Asr, Alireza, Faramarzi, A., & Javadi, A. A. (2010). A new approach for prediction of the stability of soil and rock slopes. Engineering Computations (Swansea, Wales), 27(7), 878–893. DOI:10.1108/02644401011073700

[43] Ahangar-Asr, A., Faramarzi, A., Mottaghifard, N., & Javadi, A. A. (2011). Modeling of permeability and compaction characteristics of soils using evolutionary polynomial regression. Computers and Geosciences, 37(11), 1860–1869. DOI: 10.1016/j.cageo.2011.04.015

[44] Ghanizadeh, A., Heidarabadizadeh, N., Ziaie, A. (2021). Modeling of Flow Number of Asphalt Mixtures Using Evolutionary polynomial Regression (EPR) Method. Journal of Transportation Research, 18(3), 15-28. DOI: 10.22034/tri.2021.108196

[45] Ghanizadeh, A., Delaram, A. (2021). Development of Predictting Model for Clay Subgrade Soil Resilient Modulus based on the Results of Cone Penetration Test using Evolutionary Polynomial Regression Method. Civil Infrastructure Researches, 7(1), DOI: 10.22091/cer.2021.7122.1267

[46] Karimpour-Fard, M., Lashteh Neshaei, M., Karimnader-Shalkouhi, S. (2018). Evolutionary Polynomial Regression-Based Models to Estimate Stability of Gravity Hunched Back Quay Walls. AUT Journal of Civil Engineering, 2(1), 79-86. DOI: 10.22060/ajce.2018.13198.5250

[47] Shahin, M. A. (2015). Use of evolutionary computing for modelling some complex problems in geotechnical engineering. Geomechanics and Geoengineering, 10(2), 109-125. DOI: 10.1080/17486025.2014.921333

[48] Ghorbani, A., & Hasanzadehshooiili, H. (2018). Prediction of UCS and CBR of microsilica-lime stabilized sulfate silty sand using ANN and EPR models; application to the deep soil mixing. Soils and Foundations, 58(1), 34-49. DOI: 10.1016/j.sandf.2017.11.002

[49] Shariatmadari, N., Hasanzadehshooiili, H., Ghadir, P., Saeidi, F., & Moharami, F. (2021). Compressive Strength of Sandy Soils Stabilized with Alkali-Activated Volcanic Ash and Slag. Journal of Materials in Civil Engineering, 33(11), 04021295. DOI: 10.1061/(asce)mt.1943-5533.0003845

[50] Giustolisi, O., & Savic, D. A. (2006). A symbolic data-driven technique based on evolutionary polynomial regression. Journal of Hydroinformatics, 8(3), 207-222, DOI: 10.2166/hydro.2006.020b

[51] Goldberg, D. E., & Holland, J. H. (1988). Genetic algorithms and machine learning. Machine learning, 3(2), 95-99.

[52] Balf, M. R., Noori, R., Berndtsson, R., Ghaemi, A., & Ghiasi, B. (2018). Evolutionary polynomial regression approach to predict longitudinal dispersion coefficient in rivers. Journal of Water Supply: Research and Technology-Aqua, 67(5), 447-457, DOI: 10.2166/aqua.2018.021

[53] Ahangar-Asr, A., Faramarzi, A., Javadi, A. A., & Giustolisi, O. (2011). Modelling mechanical behaviour of rubber concrete using evolutionary polynomial regression. Engineering Computations, 28(4): 492-507, DOI: 10.1108/02644401111131902

[54] Khandelwal, M., & Singh, T. (2011). Predicting elastic properties of schistose rocks from unconfined strength using intelligent approach. Arabian Journal of Geosciences, 4(3-4), 435-442, DOI: 10.1007/s12517-009-0093-6

[55] Goodarzi, A., & Moradloo, A. (2017). Effect of curing temperature and SiO2-nanoparticles on the engineering properties of lime treated expansive soil. Modares civil engineering journal, 17(3), 132-144.

[56] Harichane, K., Ghrici, M., & Kenai, S. (2011). Effect of curing time on shear strength of cohesive soils stabilized with combination of lime and natural pozzolana. International Journal of Civil Engineering, 9(2): 90-96

[57] Ghanizadeh, A. R., Yarmahmoudi, A., & Abbaslou, H. (2020). Mechanical properties of low plasticity clay soil stabilized with iron ore mine tailing and Portland cement. Journal of Mining and Environment, 11(3), 837-853.

[58] Laucelli, D., Berardi, L., Doglioni, A., & Giustolisi, O. (2012). EPR-MOGA-XL: an excel based paradigm to enhance transfer of research achievements on data-driven modeling. Paper presented at the Proceedings of 10th international conference on hydroinformatics HIC, 14-18

[59] Ghorbani, A., & Salimzadehshooiili, M. (2019). Stabilization of sandy soil using cement and RHA reinforced by Polypropylene fiber. Modares Civil Engineering Journal, 18(5), 165-176.

[60] Kogbara, R. B., & Al-Tabbaa, A. (2011). Mechanical and leaching behaviour of slag-cement and lime-activated slag stabilised/solidified contaminated soil. Science of the Total Environment, 409(11), 2325-2335, DOI: 10.1016/j.scitotenv.2011.02.037

[61] Al-Dabbas, M. A., Schanz, T., & Yassen, M. J. (2012). Proposed engineering of gypsiferous soil classification. Arabian Journal of

Geosciences, 5(1), 111-119, DOI: 10.1007/s12517-010-0183-5

[62] Dhar, S., & Hussain, M. (2021). The strength and microstructural behavior of lime stabilized subgrade soil in road construction. International Journal of Geotechnical Engineering, 15(4), 471-483. DOI:10.1080/19386362.2019.1598623

[63] Boz, A., Sezer, A., Özdemir, T., Hızal, G. E., & Azdeniz Dolmacı, Ö. (2018). Mechanical properties of lime-treated clay reinforced with different types of randomly distributed fibers. Arabian Journal of Geosciences, 11(6). DOI:10.1007/s12517-018-3458-x

[64] Remesan, R., Shamim, M., & Han, D. (2008). Model data selection using gamma test for daily solar radiation estimation. Hydrological processes, 22(21), 4301-4309, DOI: 10.1002/hyp.7044